



# 36TH INTERNATIONAL CONFERENCE ON COASTAL ENGINEERING 2018

Baltimore, Maryland | July 30 – August 3, 2018

*The State of the Art and Science of Coastal Engineering*

## Effects of Hyperconcentration-Related Drag Reduction on Tidal Propagation in the Qiantang Estuary

Wei LI and Zhenghua Su

*Ocean College, Zhejiang University, China*

**Presenter: Weiming WU, PhD**

James K. Edzwald Endowed Professor, *Clarkson University, Potsdam, NY, USA*



# CONTENTS

- **1 INTRODUCTION**
- **2 TIDAL-WAVE ANALYTICAL MODEL**
- **3 ANALYTICAL MODEL APPLICATION IN THE QIANTANG ESTUARY**
- **4 MATHEMATICAL MODELLING**
- **5 CONCLUSIONS**



# 1 BACKGROUND

In recent decade, hyperconcentration-related drag reduction has received more and more attention in the study of rivers and estuaries. Such as



Drag reduction



**The downstream peak discharge increase of hyperconcentrated floods in the Yellow River:** the later part of the flood may be accelerated by the hyperconcentration-induced drag reduction, and catch up the front part resulting an increasing discharge peak.

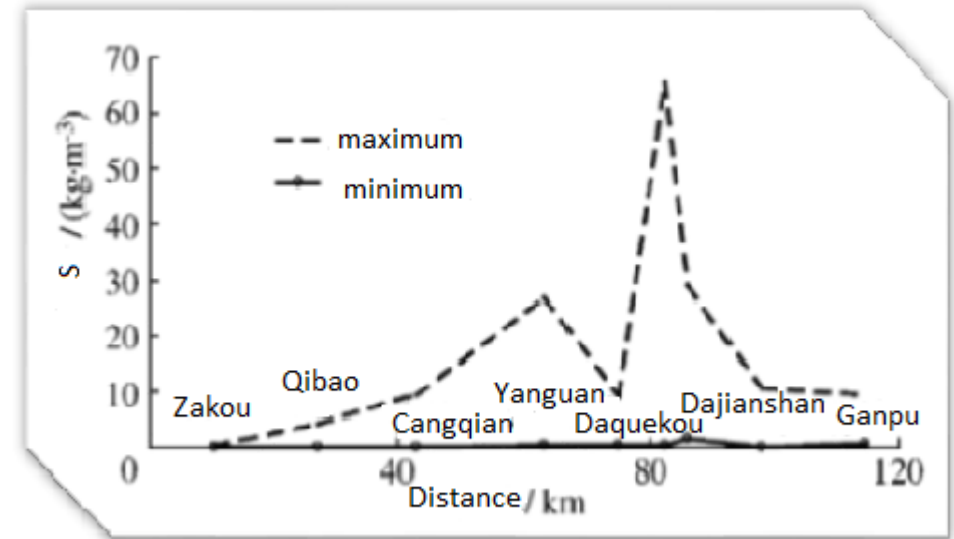
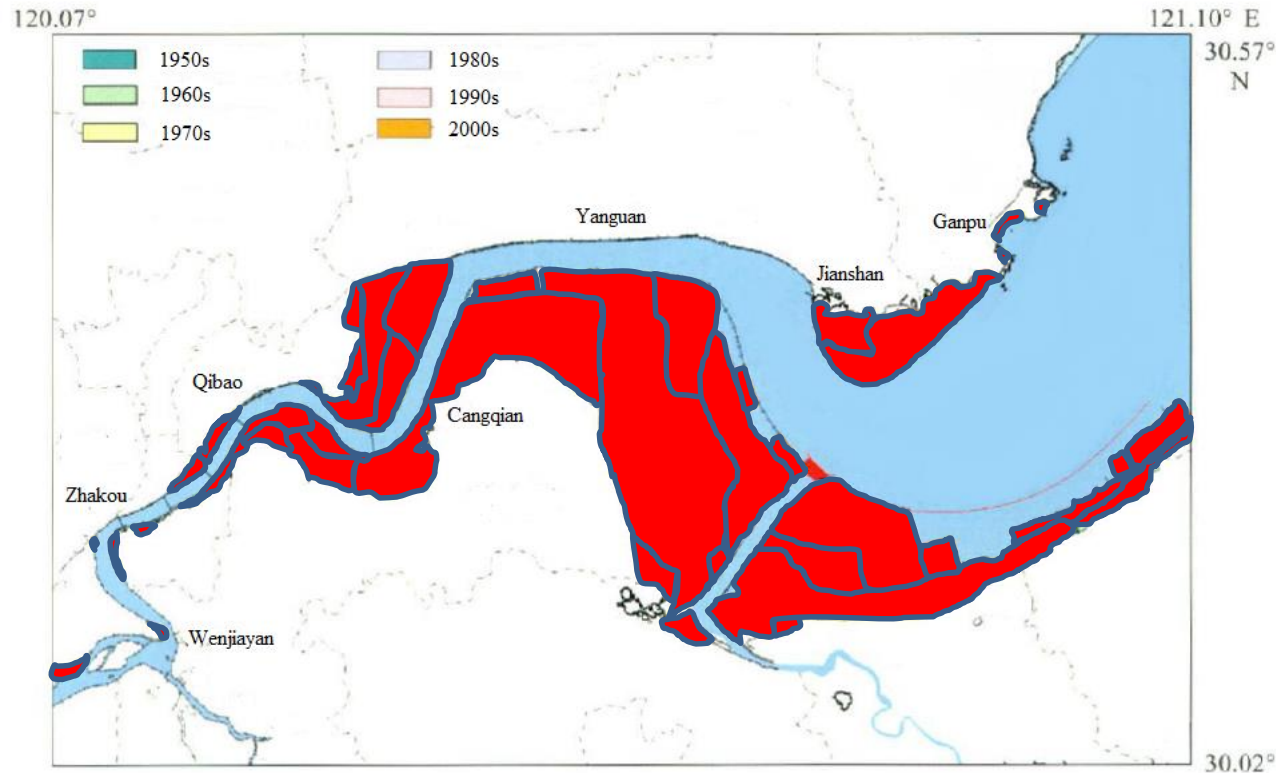
**Tidal range increase:** based on the long-term observations of the European tide-dominated estuaries, Winterwerp and Wang (2013) suggested that besides the river engineering works which largely changed the estuarine topography, the hyperconcentration-related drag reduction also played a vital role in the increase of tidal range.





# 1 BACKGROUND

Land reclamation in the past decades have greatly changed the configuration of the Qiantang Estuary which are featured by relatively high concentration of fine sediments. Tidal ranges have been observed to increase in some parts of the Qiantang Estuary after land reclamation.



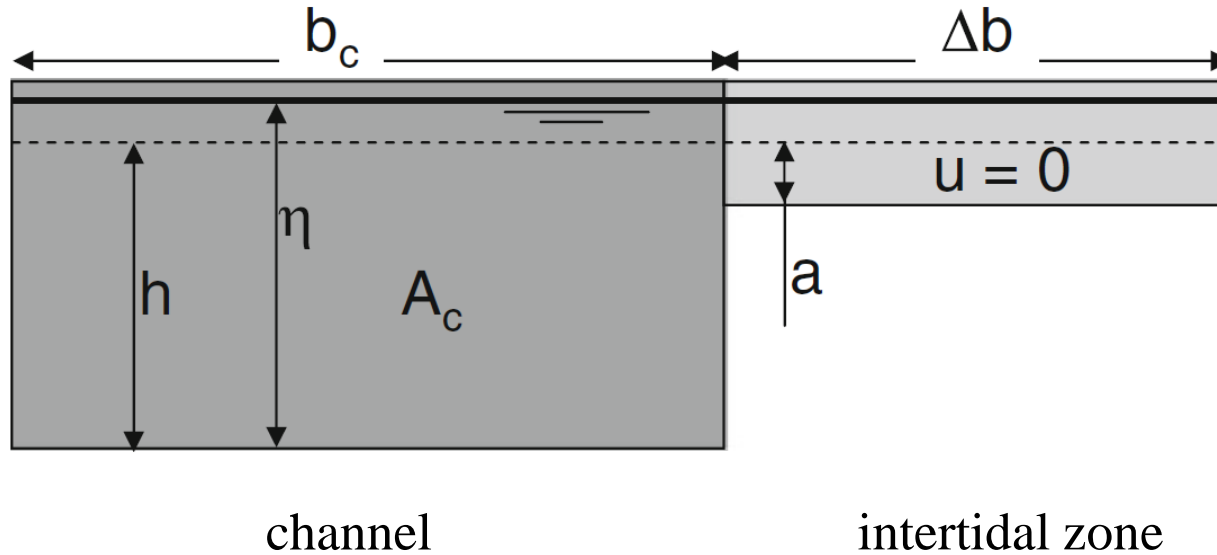
**Does the hyperconcentration-related drag reduction play a role in those tidal range increase?**



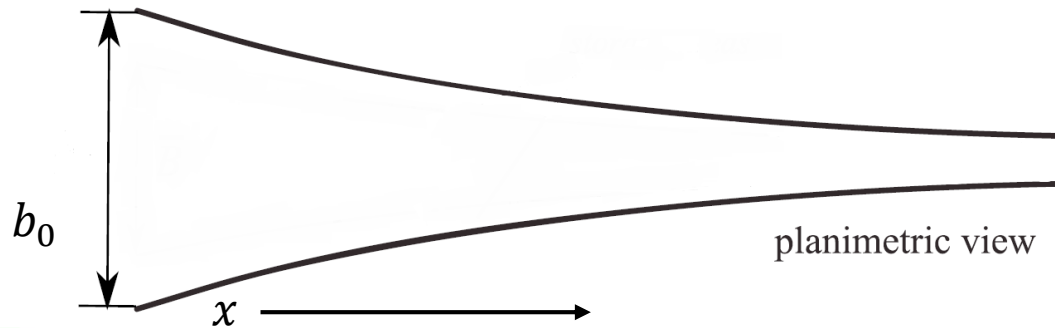
# 2 TIDAL-WAVE ANALYTICAL MODEL

## 2.1 SKETCH OF ESTUARINE GEOMETRY

Cross-section



Plan view



Assume the estuary width varies as:

$$b_c = b_0 \exp(-x/L_b)$$

$x$  — distance to the river mouth

$L_b$  — estuarine convergence length

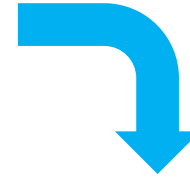


# 2 TIDAL-WAVE ANALYTICAL MODEL

## 2.2 GOVERNING EQUATIONS AND ANALYTICAL SOLUTIONS

### 1 Assumptions:

- Neglecting advection, diffusion;  $\frac{\partial h}{\partial x} = 0$



### 2 1D shallow water mass and momentum conservation equations:

Winterwerp and Wang (2013) linear friction model

$$\frac{\partial \eta}{\partial t} + \frac{A_c}{b_c + \Delta b} \frac{\partial u}{\partial x} - \frac{A_c}{b_c + \Delta b} \frac{u}{L_b} = 0$$
$$\frac{\partial u}{\partial t} + g \frac{\partial \eta}{\partial x} + \frac{ru}{h} = 0$$

Present non-linear friction model

$$\frac{\partial \eta}{\partial t} + \frac{A_c}{b_c + \Delta b} \frac{\partial u}{\partial x} - \frac{A_c}{b_c + \Delta b} \frac{u}{L_b} = 0$$
$$\frac{\partial u}{\partial t} + g \frac{\partial \eta}{\partial x} + g \frac{u|u|}{C^2 h} = 0$$

### 3 The above solutions are harmonic functions:

$$\eta(x, t) = h + a_0 e^{i(\omega t - kx)}$$
$$u(x, t) = U_0 e^{i(\omega t - kx - \varphi)}$$

at the distance  $x$ , the relative tidal amplitude  $a(x)/a_0 = e^{k_i x}$



# 2 TIDAL-WAVE ANALYTICAL MODEL

## 2.2 GOVERNING EQUATIONS AND ANALYTICAL SOLUTIONS

### 4 Uniform form of the analytical solution of the two models:

$$k_i = \frac{1}{2L_b} \left\{ 1 \mp \frac{1}{2} \left[ 2\sqrt{(\Lambda_e - 1)^2 + (\Lambda_e r_*)^2} - 2(\Lambda_e - 1) \right]^{\frac{1}{2}} \right\}$$

$\Lambda_e$  is estuarine converging index

$$\Lambda_e = \frac{b_c + \Delta b}{b_c} \frac{4L_b \omega^2}{gh}$$

$k_i$  is imaginary wave number

Relative tidal range

$$a(x)/a_0 = e^{k_i x}$$

Tidal range variations in the estuary

The essential difference is the calculation of dimensionless friction  $r_*$  :

Linear friction model-**maximum velocity**

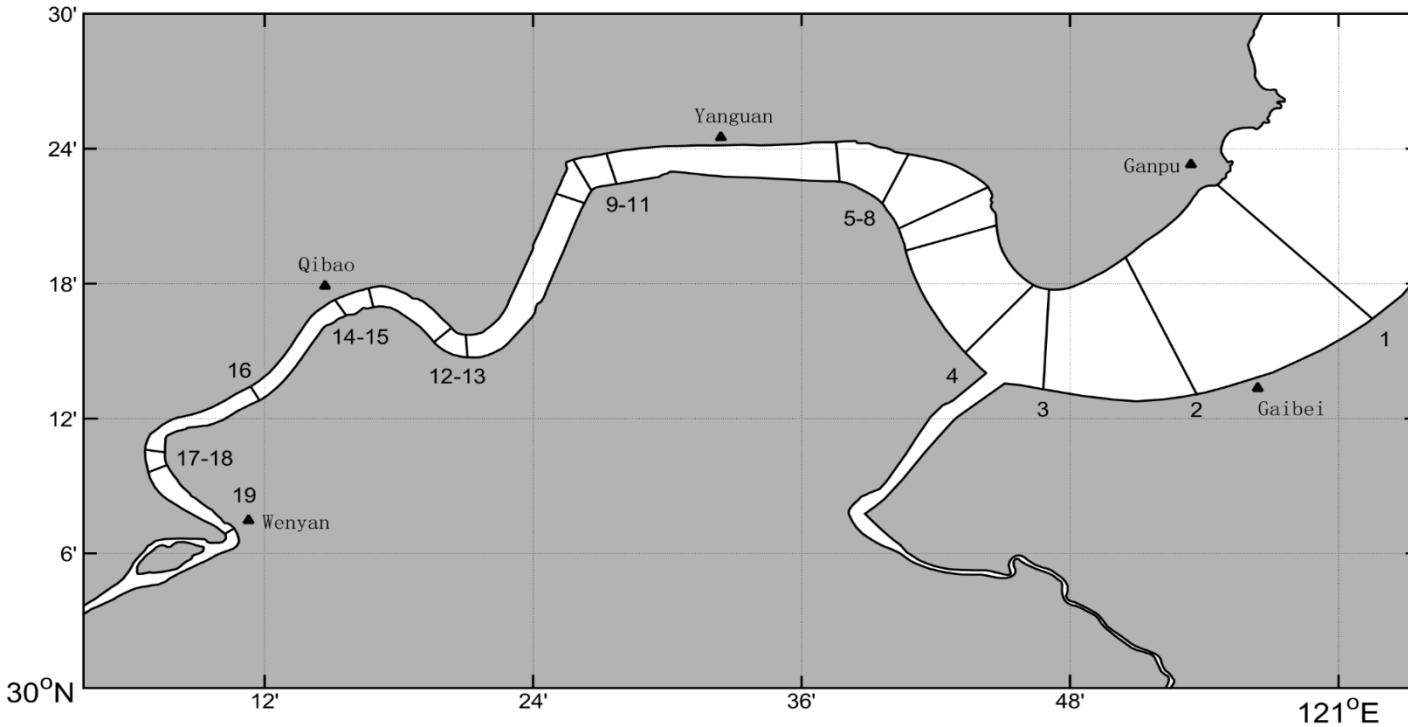
Non-linear friction model-**mean velocity**





# 3 ANALYTICAL MODEL APPLICATION IN THE QIANTANG ESTUARY

## 3.1 SUB-REACH DIVISIONS AND PARAMETER SETTINGS



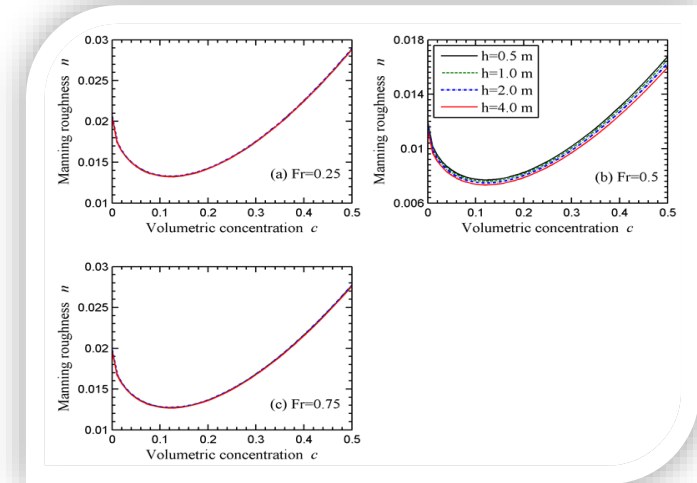
### Friction calculation

#### (1) Clear water condition

$$C = 18 \log(12 h/k_s)$$

#### (2) Hyperconcentration-related drag reduction

$$n = \frac{h^{\frac{1}{6}}}{\sqrt{g}} c_n \frac{\delta_*}{h} \left\{ 0.49 \left( \frac{\delta_*}{h} \right)^{0.77} + \frac{3\pi}{8} \left( 1 - \frac{\delta_*}{h} \right) \left[ \sin \left( \frac{\delta_*}{h} \right)^{0.2} \right]^5 \right\}^{-1}$$



#### (3) Bed-material dependent friction

No.	1-2	2-16	16-19
$\Gamma_*$	4	3	5

- Semi-diurnal T=12.42h
- Water depth, velocity, sediment concentration, median diameter from the field observations

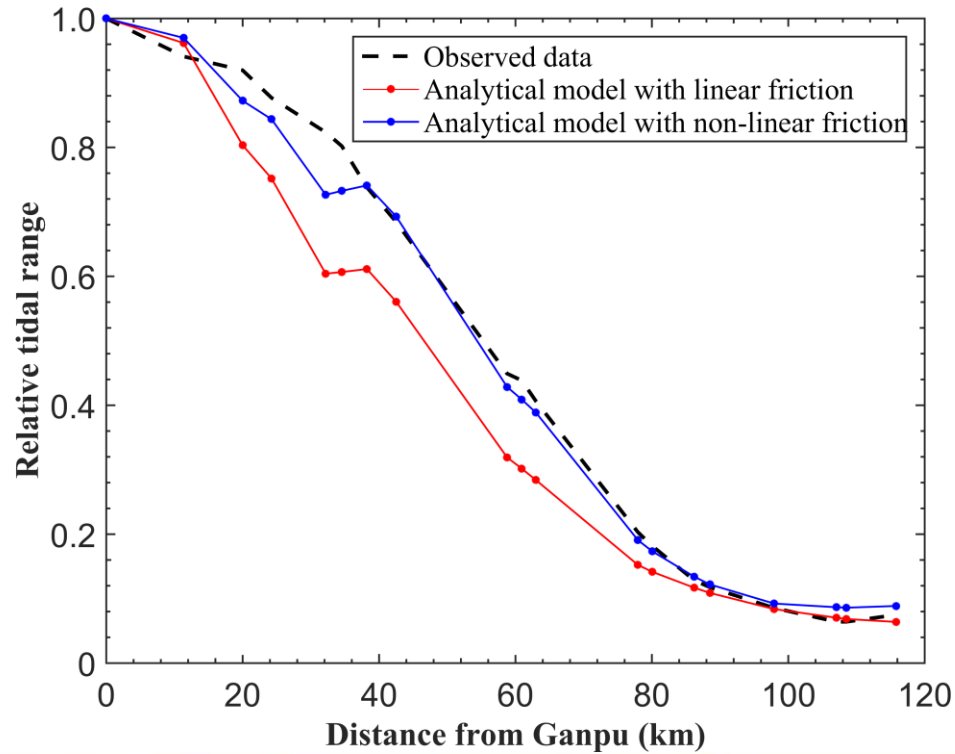




# 3 ANALYTICAL MODEL APPLICATION IN THE QIANTANG ESTUARY

## 3.2 ANALYTICAL RESULTS

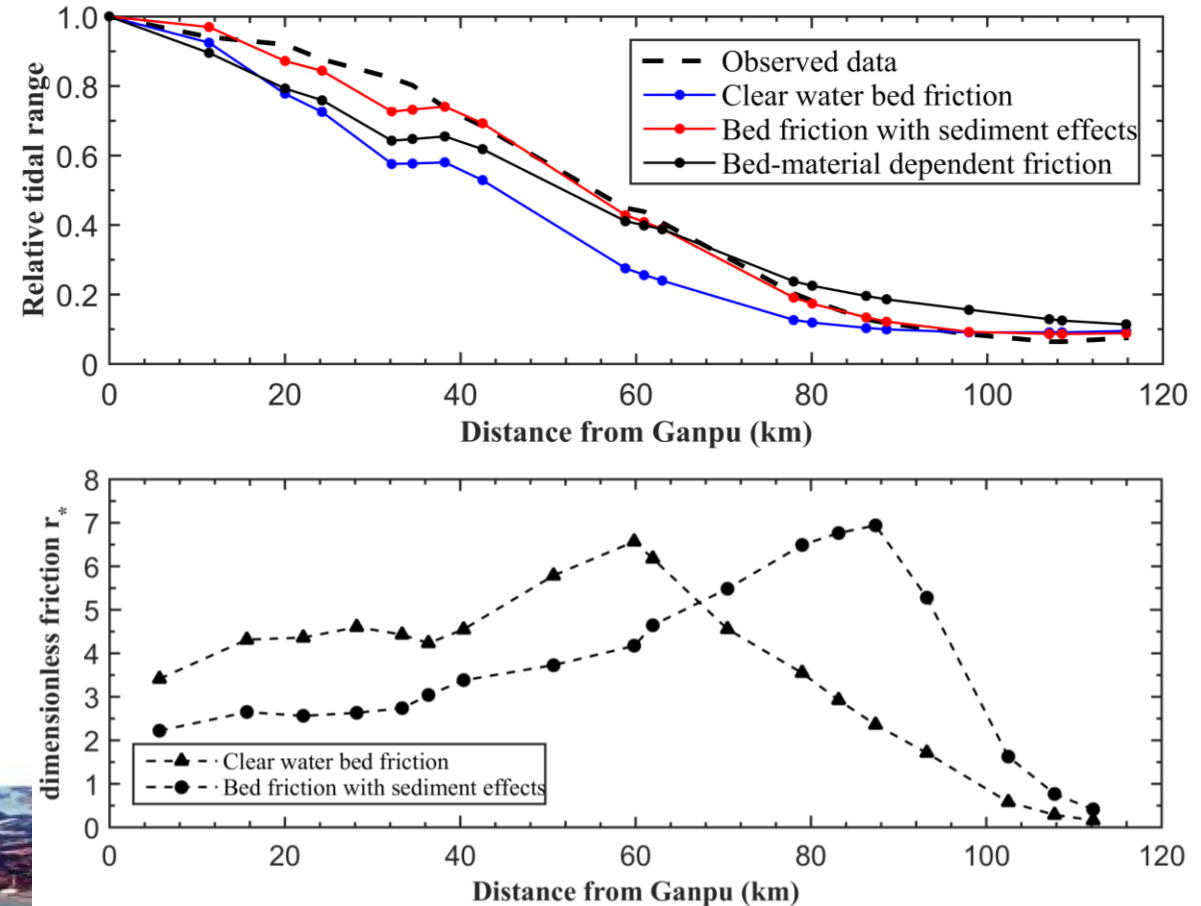
### (1) Comparison of linear and non-linear friction models



Hyperconcentration-related drag reduction



### (2) Comparison of different friction methods for non-linear friction model



# 4 MATHEMATICAL MODELLING

## 4.1 2D DEPTH-AVERAGED MODEL

### (1) Governing equations

$$\frac{\partial h}{\partial t} + \frac{\partial(hu)}{\partial x} + \frac{\partial(hv)}{\partial y} = 0$$

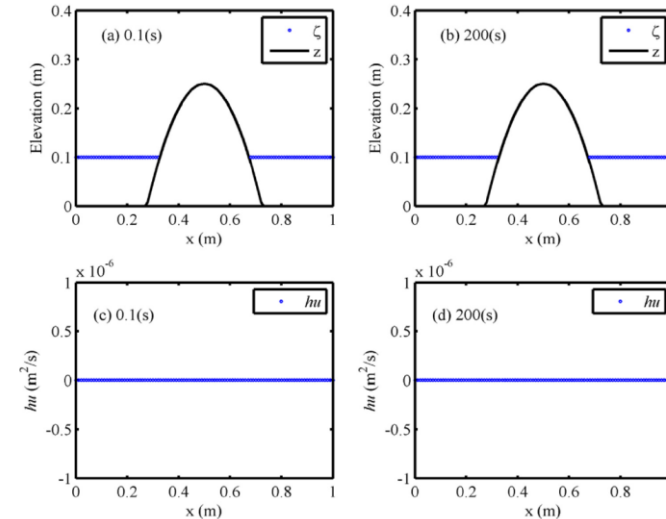
$$\frac{\partial(hu)}{\partial t} + \frac{\partial(hu^2 + 0.5gh^2)}{\partial x} + \frac{\partial(huv)}{\partial y} = gh(S_{0x} - S_{fx})$$

$$\frac{\partial(hv)}{\partial t} + \frac{\partial(huv)}{\partial x} + \frac{\partial(hv^2 + 0.5gh^2)}{\partial y} = gh(S_{0y} - S_{fy})$$

### (2) Numerical methods

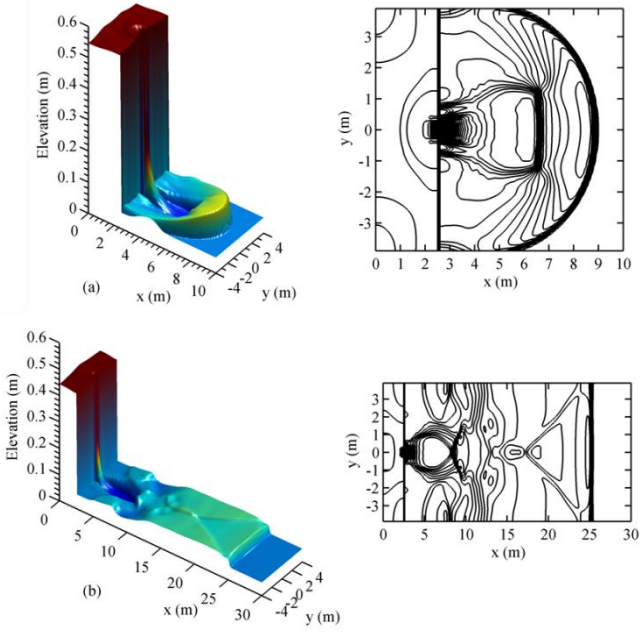
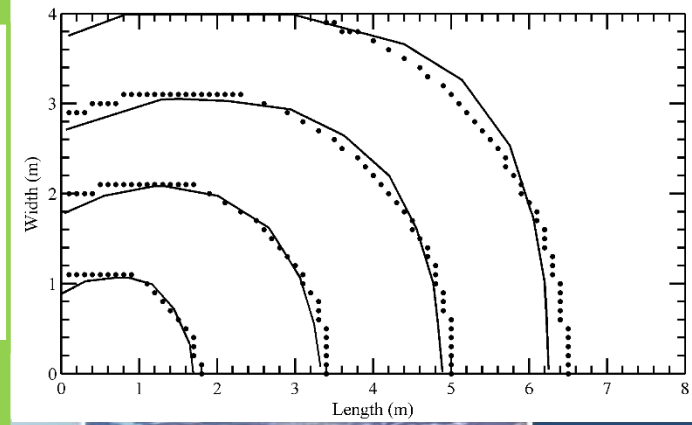
- Cartesian grid
- UFORCE scheme for flux computing
- 2<sup>nd</sup> order Runge-Kutta for source terms
- C-property

2<sup>nd</sup> order accuracy in space and time



C-property

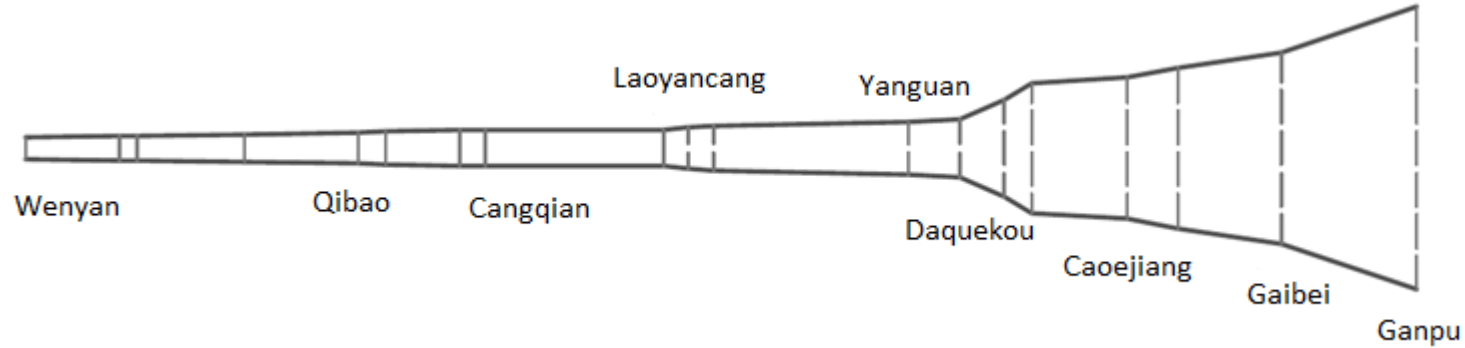
### Shock wave capturing



# 4 MATHEMATICAL MODELLING

## 4.2 MODEL SET-UP

### (1) Sketch of the Qiantang Estuary



### (2) Computational region

Computational domain  $115.8\text{km} \times 20.4\text{km}$ , grid size  $100\text{m} \times 100\text{m}$ , 238960 grids

### (3) Initial and boundary conditions

Upstream end: constant water level, downstream end: periodic water level

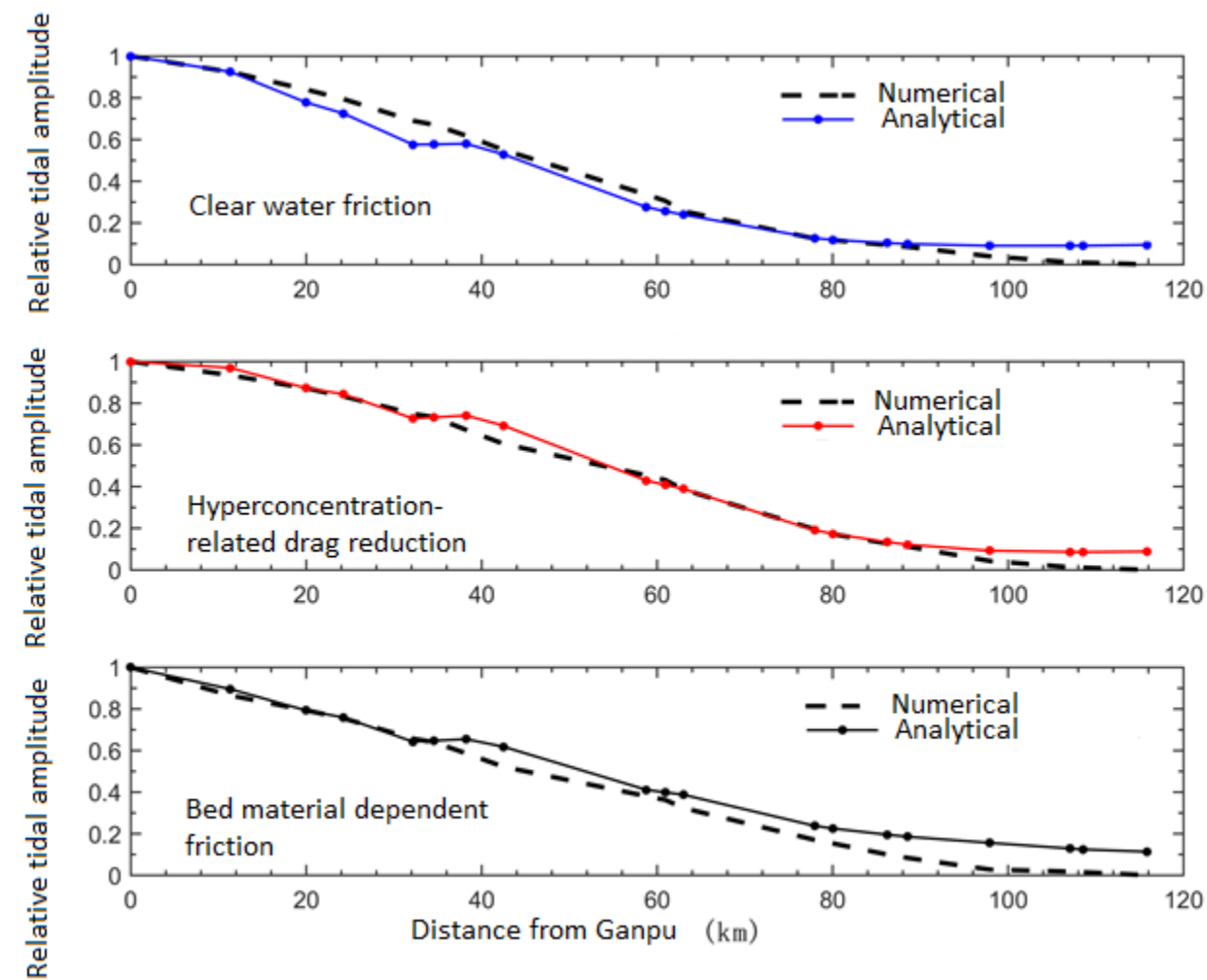
Initially static water, bed level equals to initial water level subtracting water depth



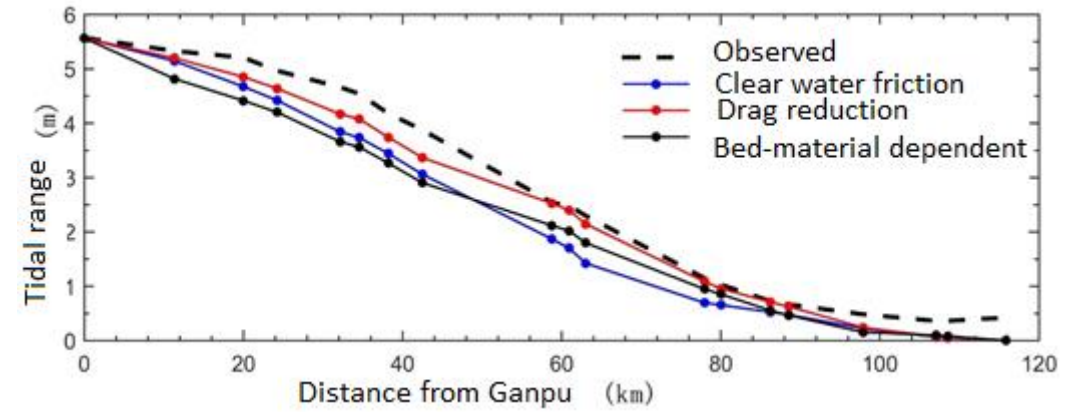
# 4 MATHEMATICAL MODELLING

## 4.3 MODEL RESULTS

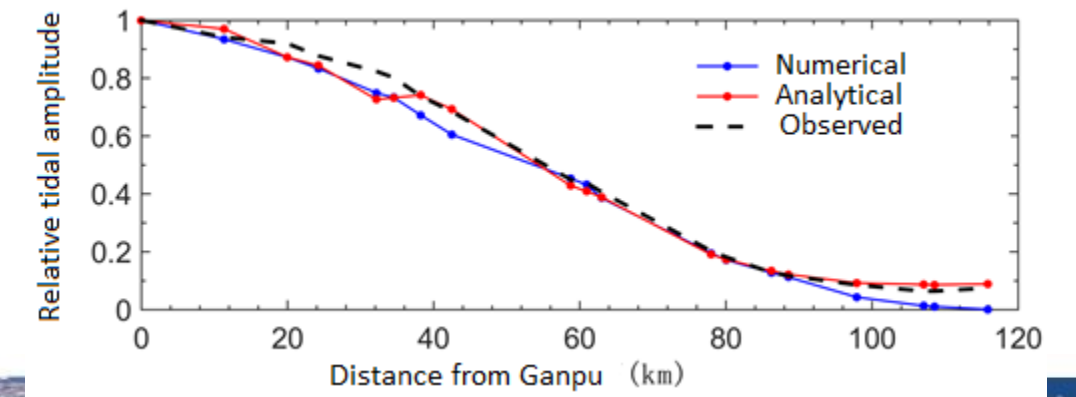
### (1) Comparison of analytical and numerical results



### (2) Numerical results of different friction methods against observations



### (3) Comparison of analytical and numerical results for drag reduction methods against observations

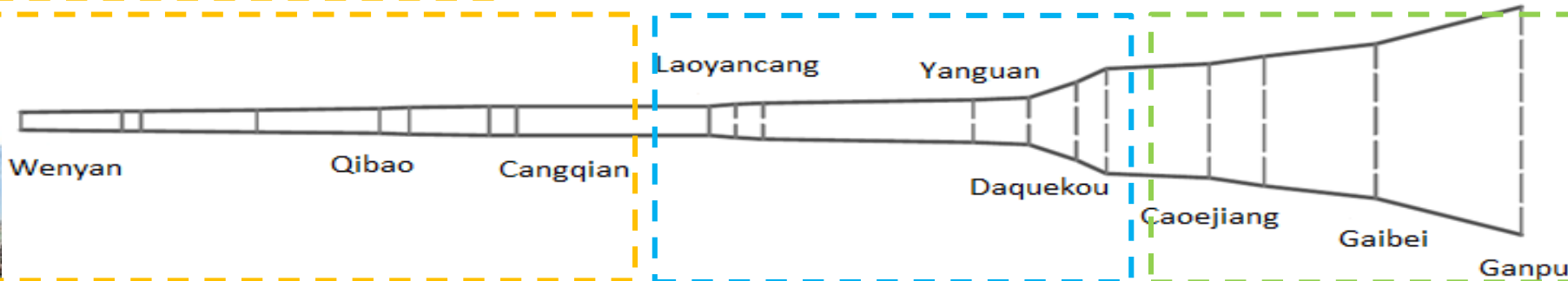
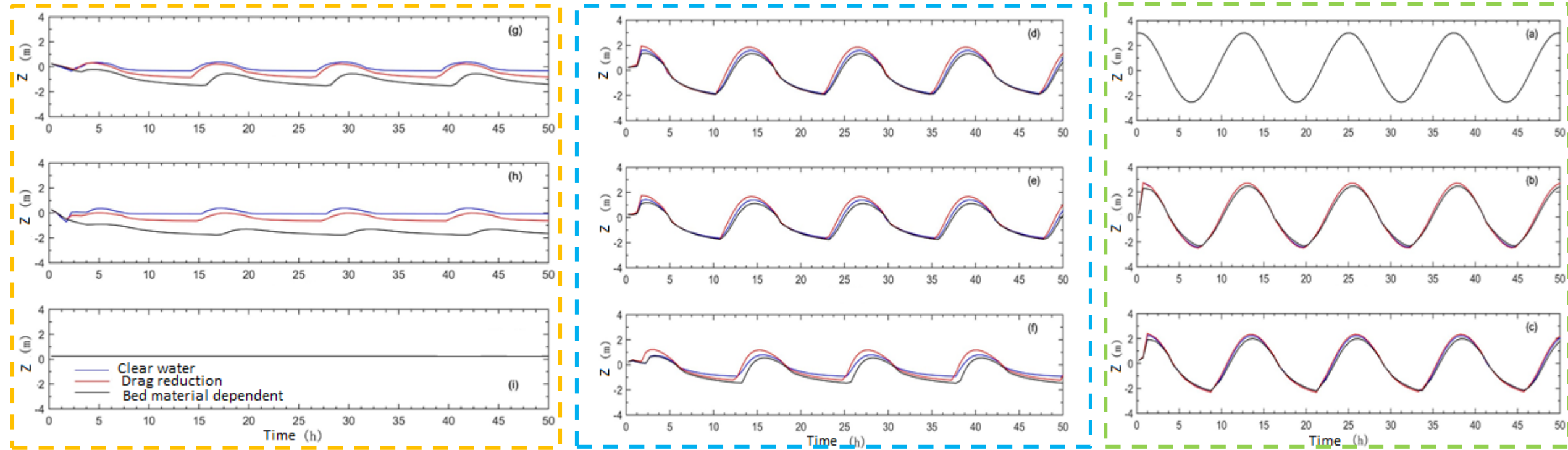




# 4 MATHEMATICAL MODELLING

## 4.3 MODEL RESULTS

### (4) Time evolution of water level at representative stations



# 5 CONCLUSIONS

- The accuracy of the tidal range prediction in an analytical model is obviously improved when a non-linear friction using mean flow velocity replaces a linear friction using maximum flow velocity.
- Regarding high sediment-laden estuaries such as the Qiantang Estuary, hyperconcentration-related drag reduction may explain the extremely small bed friction calibrated in traditional mathematical modelling, providing a more physical way for accurate prediction of tidal waves.
- The good fit of analytical and numerical results of drag reduction to the observed tidal ranges not only implies its importance, but also demonstrates the successful extension of the Yellow River drag reduction formula to the Qiantang Estuary.



# THANK YOU FOR LISTENING!



**36TH INTERNATIONAL CONFERENCE  
ON COASTAL ENGINEERING 2018**  
Baltimore, Maryland | July 30 – August 3, 2018